

# Search for mobilised dust during operations with equipment for remote handling in JET with ITER-like wall

M Rubel<sup>1</sup> , A Widdowson<sup>2</sup> , E Fortuna-Zaleśna<sup>3</sup>, C Ayres<sup>2</sup>, M Berry<sup>2</sup>, M Burford<sup>2</sup>, S Collins<sup>2</sup>, P Macheta<sup>2</sup> and JET Contributors<sup>4</sup>

<sup>1</sup>Royal Institute of Technology (KTH), SE-1044 Stockholm, Sweden

<sup>2</sup>CCFCE, Culham Science Centre, Abingdon, OX14 3DB, United Kingdom

<sup>3</sup>Warsaw University of Technology, 02-507 Warsaw, Poland

E-mail: [rubel@kth.se](mailto:rubel@kth.se)

Received 25 June 2019, revised 9 October 2019

Accepted for publication 21 October 2019

Published 6 March 2020



CrossMark

## Abstract

Accumulation of dust on the equipment for remotely handled (RH) operations was studied in JET with the ITER-like wall (JET-ILW) during the shutdown period following the third ILW campaign. The topic is connected to licensing procedures for ITER: the need to assess risks related to the external transfer of beryllium and radioactive matter with tritium and activation products. Ten adhesive carbon pads were placed in different locations on the robotic arm operated in-vessel for 672 h. Also air samplers were used during the RH operation and smear tests of the RH boom were performed to quantify specific contamination levels by beryllium and tritium. Dust morphology was determined by microscopy techniques. The areal density of dust varies at different sticker position on the boom. On some parts (e.g. ‘wrists’ of the robot) the density of particles exceeds 1000 per mm<sup>2</sup>. Their morphology is very diverse but most collected objects originate from the construction material (aluminium) of the RH equipment itself. The accumulation of Be- and W-based particles is negligible. The study confirms earlier experimental evidence that Be-rich co-deposits (and also W coatings on CFC) adhere well to plasma-facing components and they are not easily mobilised.

Keywords: JET-ITER like wall, dust, beryllium, remote handling, licensing

(Some figures may appear in colour only in the online journal)

## 1. Introduction

The presence of dust in fusion devices is an unavoidable consequence of mechanical in-vessel operations and material erosion-deposition processes. Risks associated with the generation and accumulation of dust particles originating from erosion of plasma-facing components (PFC) in controlled fusion devices have been identified and discussed for the last two decades. For that reason comprehensive studies of dust have been carried out and regularly reported [1–8]. The issue was especially severe in carbon-wall tokamaks where thick layers of co-deposits were formed and then peeled-off [9, 10].

Great seriousness of fuel retention and dust formation was fully recognised after the deuterium-tritium campaign in JET with carbon walls (JET-C) [9–12]. The extrapolation to reactor conditions led to conclusions that tritium inventory and quantities of dust would make the safe and economically viable operation not possible. This, in turn, had major consequences for the wall technology: beryllium and tungsten in the JET tokamak with the ITER-Like Wall (JET-ILW) [13, 14], followed by the decision on the elimination of carbon components from the ITER divertor [15].

Regarding dust, there were already some indications from ASDEX Upgrade with tungsten-coated PFC [16] that the amount of generated particles was decreased when compared to the situation with carbon wall [5, 17]. Operation of JET-ILW has clearly proven low amounts of dust in the

<sup>4</sup> See author list of E Joffrin *et al* 2018 27th IAEA Fusion Energy Conf. (India).

presence of metal PFC: around 1 g per campaign (19–23 h plasma operation) [18–22] in comparison to over 200 g removed by vacuum cleaning of the divertor after the last JET-C operation [9]. In the case of metallic wall components one has to take into account metal melting and splashing and also arcing as possible sources of dust [5, 6, 18, 22–25]. In parallel to research concentrated on the amount, size and morphology of particles sampled and retrieved by various means from vacuum vessels, there have been also studies—both experiment and theory/modelling—on dust mobilisation and motion during plasma discharges [4, 26–29].

From the safety point of view there is also another aspect which is to be thoroughly addressed in the licensing procedures: dust mobilisation and transfer outside the vacuum vessel. This issue is connected with beryllium and radioactive matter containing tritium and activation products. Therefore, on the direct request from the ITER Organisation, the accumulation of dust on the remotely handled (RH) [30] equipment was studied in JET with the ITER-like wall (JET-ILW) during the shutdown after the third ILW campaign. The exercise carried out for the first time-ever aimed at answering three basic questions: what, how much and where on the arm is deposited and transferred outside the vessel? Specific emphasis has been given to the transfer and sticking of beryllium and tungsten particles, and to the contamination by tritium and beryllium of the RH equipment and in-vessel air.

## 2. Experimental

To facilitate the task, ten adhesive carbon pads (stickers of 1 inch in diameter) were placed in different locations along the robotic arm (boom) and on the multifunctional robot (Mascot). A drawing in figure 1(a) shows schematically the structure of the multi-segment boom. It also informs about the extent in remotely controlled operations ensuring access to each place in the entire tokamak chamber. The location sector A-0/A-1 is in the tunnel between the boom enclosure. Joint A1 reaches as far as the vessel port. There is a skirt at the boom enclosure door which rubs on both the upper and lower surfaces of the plastic gaiter covering the metal structure. The equipment is made of aluminium (Al) and boron nitride (BN) is used as a lubricant of joints [31]. Details of the construction and the location of stickers on the gaiter protecting the boom are presented in figure 1(b). The location of samples was thoroughly planned and selected to ensure maximum outcome. Possible contamination and even cross-contamination by different sources have been taken into account; details are listed in table 1.

The stickers were on the equipment for nearly four months with 672 h of operation. This has allowed for collecting airborne dust. In addition, after 580 h of RH work, air samplers consisting of cellulose filtration papers were attached twice to a pump for a couple of hours on each occasion (pumping rate  $0.9 \text{ m}^3 \text{ h}^{-1}$ ). After the boom retraction, the gaiter was smeared in twelve areas (each of  $\sim 1000 \text{ cm}^2$ ) with the filtration paper to assess beryllium and tritium contamination levels at different locations.

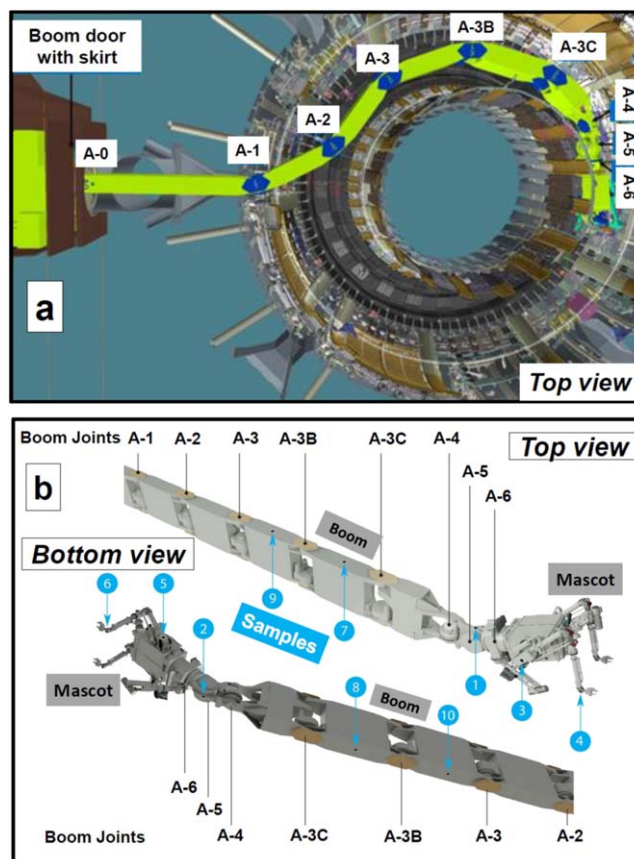


**Figure 1.** (a) Extent of boom in vessel and (b) location of carbon adhesive pads, 1–10, and boom joint numbering used to define smearing locations. Joints A-1–A-6 are shown.

Retrieval of the adhesive pads and transfer to analytical laboratories was a multi-step process. First, within the boom enclosure the pads were cut from the gaiter material and stuck into Petri dishes for transport to the JET Beryllium Handling Facility (BeHF). Then they were removed using tweezers, stuck to aluminium stubs (i.e. to standard sample holders for microscopy) and placed into individual stub holder tubes. The air flow through the slit box used was  $1800 \text{ m}^3 \text{ h}^{-1}$ , while the flow through the JET vessel was  $5000 \text{ m}^3 \text{ h}^{-1}$ . Each sample was exposed to the air flow for a few minutes only, thus corresponding to a fraction of the time of exposure on the RH boom. The individual tubes were transferred to the Warsaw University of Technology where morphology of particles was determined by means of scanning electron microscopy (SEM) and energy dispersive x-ray spectroscopy (EDS) using beryllium-sensitive detector. However, in the case of search for Be (the main aim of work), the automated SEM/EDS analyses could not be applied because the energy of the only line  $K(\alpha)\text{Be}$  is only 108 eV. As a result, Be detection in mixed materials is extremely difficult and requires very careful ‘manual’ approach [19, 20].

The cellulose filtration papers from the air samplers and gaiter smearing were analysed at Culham centre for fusion energy using a fluorescence technique to quantify beryllium contamination levels and scintillation counting to quantify tritium. For the beryllium quantification, firstly beryllium is

**Table 1.** Numbering and description of adhesive pads.

Sample number	Locations description	Rationale for sample locations on RH
1	Mascot joint: top	Highest exposure at upper surface. Would expect to see Be and/or C particles settling from in vessel environment.
2	Mascot joint; bottom	Some in vessel contamination possible. Potential for contamination during maintenance in boom enclosure.
3	Mascot arm: right	In vessel particles expected. Possible light contact with vessel wall.
4	Mascot wrist: right	Highest level of contamination expected in vicinity of in vessel operations. Contamination from maintenance possible.
5	Mascot arm: left	In vessel particles expected. Possible light contact with vessel wall.
6	Mascot wrist: left	Highest level of contamination expected in vicinity of in vessel operations. Contamination from maintenance possible.
7	Boom top surface A-3B/ A-3C	Would expect to see Be and/or C particles settling from in vessel environment. Probably small contamination.
8	Boom bottom surface A-3B/ A-3C	Fewer particles from in vessel expected. Potential for contamination during maintenance in boom enclosure if workers crawl below the boom.
9	Boom top surface A-3/A-3B	Would expect to see beryllium or carbon particles settling from in vessel environment. Probably small contamination.
10	Boom bottom surface A-3/ A-3B	Fewer particles from in vessel expected. Potential for contamination during maintenance in boom enclosure if workers crawl below the boom.

extracted from the cellulose filter paper using an ammonium difluoride solution. This is followed by a fluorescence measurement of a complex formed between beryllium ions and hydroxybenzoquinoline sulfonate (HBQS), where the HBQS + Be complex absorbs UV at 380 nm and emits at 450 nm. The amount of beryllium recovered from the filter paper is determined by the change in absorption and emission of the solution using a UV spectrometer. The tritium quantification is done by means of liquid scintillation method for measuring radiation from beta-emitting radioactive isotopes, using a scintillation cocktail consisting of solvents, surfactants and scintillators. A scintillation counter is used to measure the light produced by the chemical scintillator from which the amount of tritium in solution can be determined. The specific tritium activity ( $\text{kBq m}^{-2}$ ) and specific beryllium mass ( $\mu\text{g m}^{-2}$ ) were then calculated using the smeared area, typically  $1000 \text{ cm}^2$ . General aspects and details of procedures for handling contaminated materials have been described earlier [32].

### 3. Results and discussion

#### 3.1. Dust accumulated on adhesive stickers

A collection of micrographs and x-ray spectra in figures 2 and 3 survey data for two samples from distinctly different locations: the top surface of the boom (Sample 9) and the Mascot wrist (Sample 4), respectively. In all cases observations were performed at several places on the sticker. There are islands with a fairly high density of particles exceeding  $1000 \text{ mm}^{-2}$ . For comparison, the typical areal density of particles found on in-vessel dust monitors in JET was  $400\text{--}500 \text{ mm}^{-2}$  [22]. On all other exposed stickers one also finds species of various size and shape but the areal density is lower than on those shown above. The composition of individual grains is very

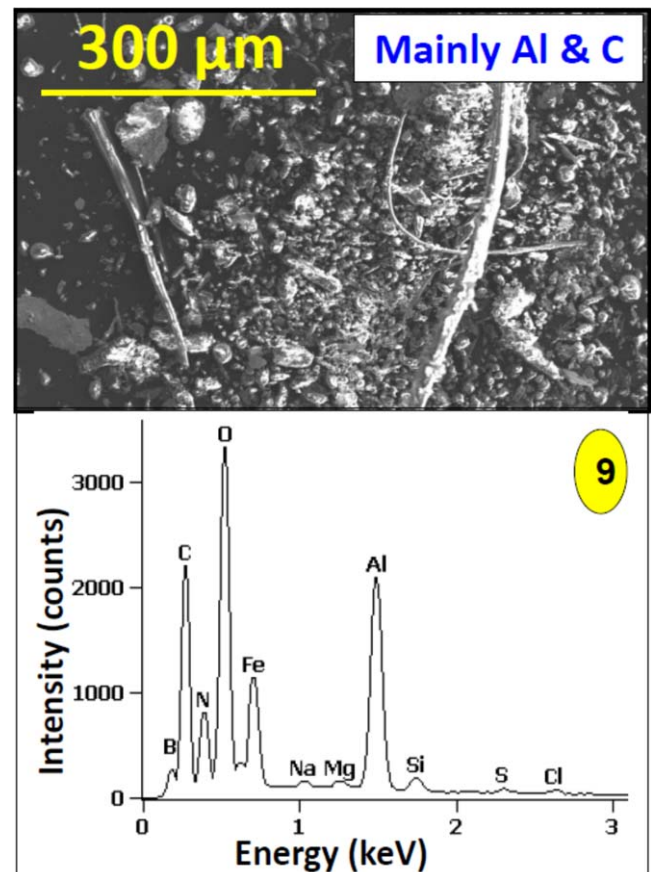


**Figure 2.** SEM image and an example of x-ray spectrum for dust particles accumulated on Sample 9 from the top surface of the boom A3-A3B.

diverse and one finds a mix of low-Z and medium-Z elements: B, C, N, O, Na, Mg, Al, Si, S, Cl, Cr, Fe, Ni. Aluminium and carbon particles constitute the majority. However, the least frequent are those particles for which the

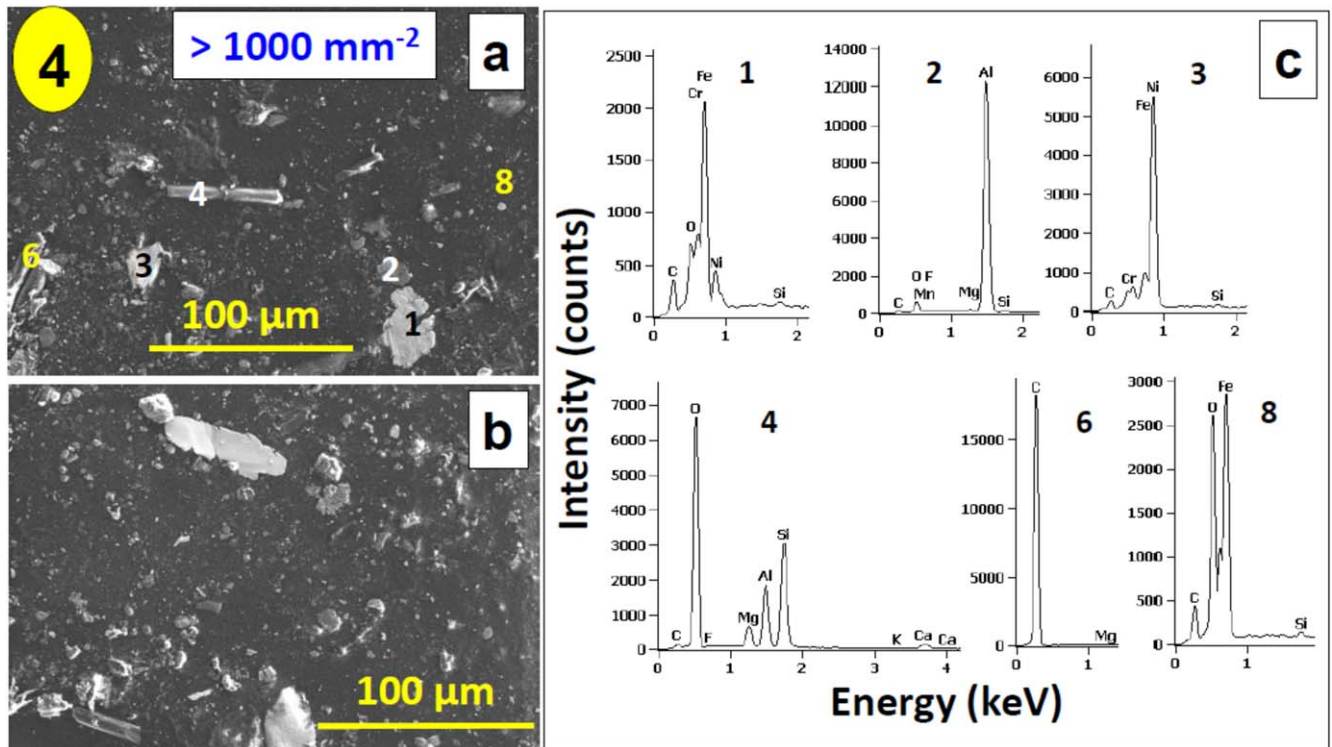


**Figure 3.** SEM and EDS data for various dust particles accumulated on Sample 4 from the right wrist of the Mascot: (a) and (b) survey images in different area; (c) x-ray spectra for selected single particles; numbers in the spectra correspond to individual grain marked in frame (a).

whole reported search had been designed and performed: (a) beryllium flakes from co-deposited layers or tiny droplets from melt-damaged limiters; (b) tungsten flakes or droplets. Only one flake of a co-deposit rich in beryllium and carbon has been identified on Sample 4 (Mascot wrist). That object with splitting strata is shown in figure 4.

It cannot be excluded that there were also some other tiny Be-rich species sticking to the pads, but one can state that the RH operation did not lead to a massive disintegration and mobilisation of co-deposits. Examples of some other particles are shown in figure 5. The iron particle in figure 5(a) is a typical piece of swarf, i.e. remnant of metal machining, either in-vessel or outside. One may infer that the copper particle most probably from the neutral beam injector, particle shown in figure 5(b), had been affected by plasma. A spongy piece in figure 5(c) is an agglomerate of many light and medium-Z impurities present in the vessel. The examination identified also a spherical iron particle resembling ball-like objects consisting of thousands of coagulated tiny tungsten flakes described in earlier works [21, 22]. In the case of tungsten only very few tiny (less than  $1\ \mu\text{m}$ ) species have been found. In general, metal particles (Fe, Ni, Cu, W) identified on various samples are of micrometre size. For reasons explained in section 2 (Experimental), the automated SEM/EDS analysis could not be performed. Up to one thousand particles were checked, but careful search for Be-rich co-deposits were performed over 70%–80% of the samples' area. From previous studies [19–22] the structure and appearance of Be co-deposits and droplets have been known, therefore, such objects could be distinguished from other particles, especially

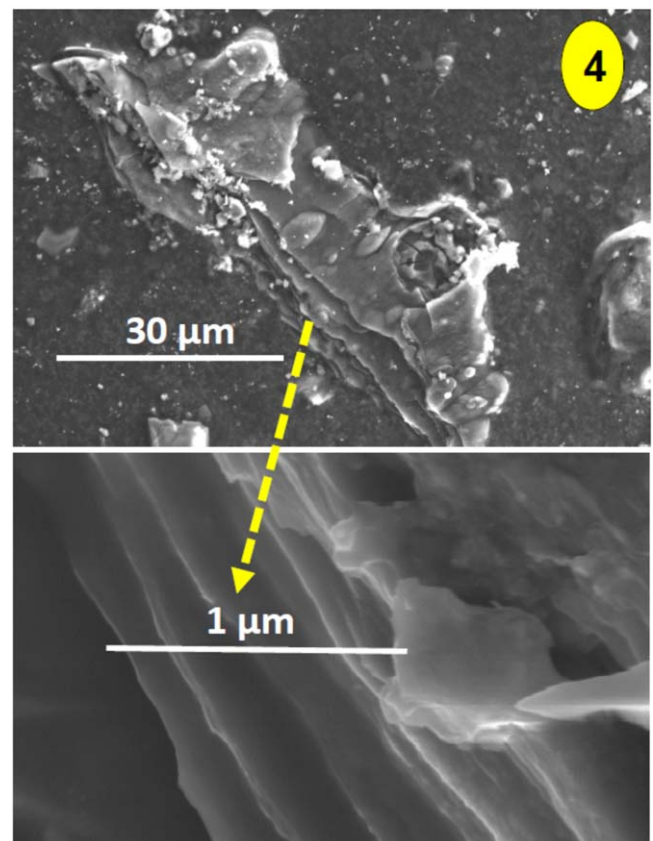


**Figure 4.** A flake of a stratified co-deposit containing mainly beryllium and carbon; a single object found on Sample 4 from the right wrist of the Mascot.

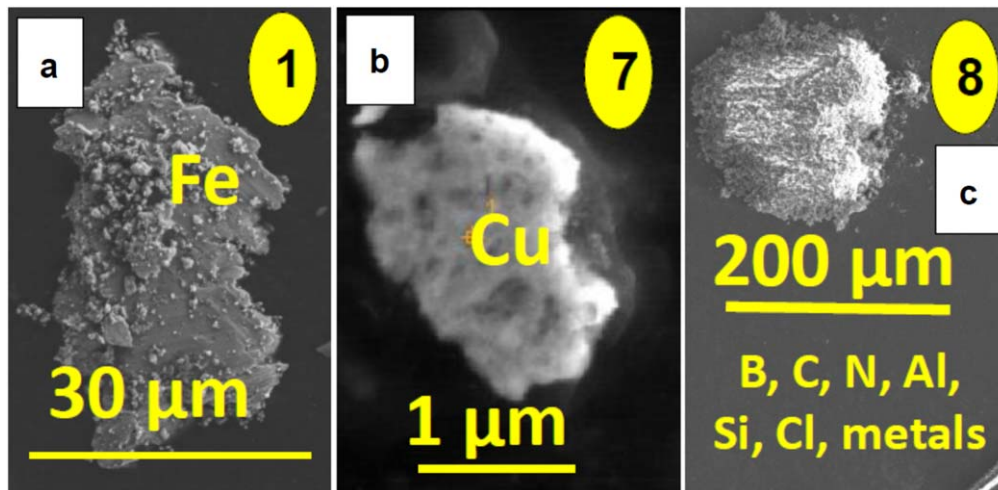


**Figure 5.** SEM images showing examples of particles identified on samples from various locations both on the boom and Mascot. Material composition and sample number is given in the frames.

**Table 2.** List of identified elements and their potential origin.

Particle and figure	Comment and quantity (%)	Potential origin
Al metal figures 2 and 3	Operation of boom creates Al particles: 70%–75%	Material of RH boom structure
B and N together figure 2	Suggests boron nitride, BN: 4%–5%	Lubricants of joints of RH boom
Carbon particles and debris figures 2–4	Carbon fibre composites and co-deposits: 20%	Debris of carbon fibre composites and legacy from carbon operations
C fabrics	Evidence of cross contamination of sampling	Personal protective clothing
C, Ca and O together	Suggests CaCO <sub>3</sub>	Unknown source
Si pieces	5–30 μm	Unknown sources
Al–Si–Mg—also a little Ca and F in mixtures figure 3	Probably ceramics: <0.1%	Ceramics used in vessel—breakages/cracking
Fe; figures 3 and 5(a)	Small bits	Machining/in- or out-vessel work
Cu; figure 5(c)	Small bits: <0.1%	Neutral beam injectors
Fe + Cr figures 2 and 3	Probably steel	Machining/in-vessel work
Ni figure 3	Probably Inconel alloy, extensively used: <1%	Machining/in-vessel work
Be + C figure 4	Only one flake showing stratified structure: <<0.1%	Peeled-off co-deposit
W	Very few tiny flakes: <0.1%	W coatings, particles found mostly in divertor, but also a few in main chamber.

from Al. However, it is also understood that the manual analysis has had an impact on the total number of examined particles and caused some uncertainty in statistical evaluation of species accumulated on the RH equipment.

Data in table 2 provide a catalogue of particle elemental composition and the most probably source of their origin. Aluminium is on the top of the list. It becomes evident that Al originates from the structural material of the RH equipment, as there are no other sources of pure Al in the vessel. Aluminium in dust samples has been noted in other analysis [22], but this is the first evidence of the source of such particles in the vessel. The presence of boron nitride is associated with the boom: a component of the lubricating agent. As explained in the table, there are several possible sources of carbon such as debris from carbon fibre composites (CFC) particles

remaining after the JET-C operation. Certain impurities (e.g. fabrics) could be accumulated on the stickers in the boom enclosure during pre- or post-operation phases. It is likely that some species were deposited during the handling of the adhesive pads, as the boom enclosure, (where the pads were initially mounted and dismantled) is a working facility, not a clean room. The origin of some species, e.g. Ca or bits of Si, has not been identified; the source remains unknown.

### 3.2. Boom gaiter contamination by beryllium and tritium

The contamination was assessed using a smearing survey procedure in which two cellulose based filter papers are rubbed across the surface to be tested; one for beryllium assessment and one for tritium measurements. The size of the

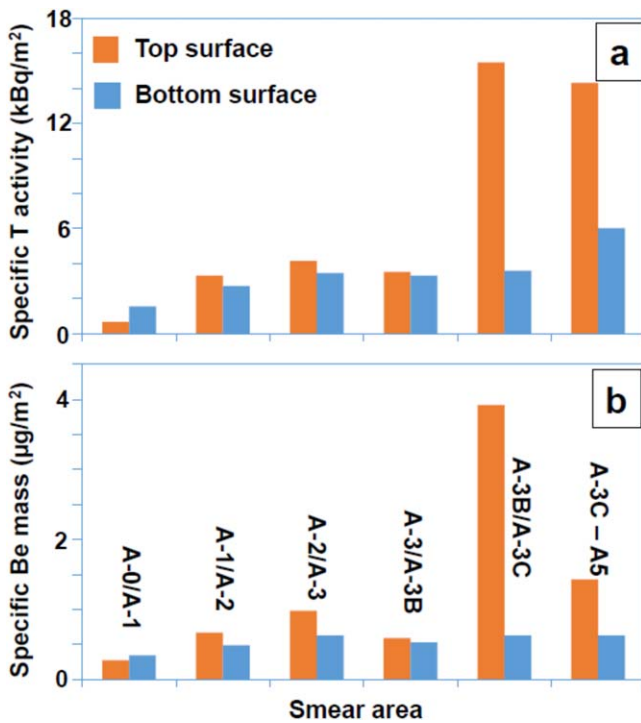


**Figure 6.** Results of smear test on the gaiter: (a) specific tritium activity and (b) specific mass of beryllium in twelve examined positions.

smear area is also recorded to enable determination of specific values of contamination per unit area. For the boom gaiter a series of Be and T smears were taken between the joints A-0/A-1, A-1/A-2 etc, along the top and bottom surfaces. The results of the smear analyses by techniques described in section 2 are shown in figures 6(a) and (b) for T and Be, respectively. They indicate that in most cases the values are higher on the upper side than the lower side, although the values on the upper side seem to be higher from A-3B to A-5. In this type of exercise it is not possible to determine the direct cause for that increase but one can consider two highly probable reasons: (a) light contact of RH (touching) with the vessel wall and (b) relative proximity to the Mascot operation area in comparison to other samples from A-0 to A-3B. In general, the contamination by beryllium is considered to be low,  $<1.5 \mu\text{g m}^{-2}$  for 91% of results and  $<4 \mu\text{g m}^{-2}$  for all results, as shown in figure 6(b). This is below the  $10 \mu\text{g m}^{-2}$  threshold used at UKAEA whereby additional controls such as personal protective equipment, personal air sampling and specified working procedures are required to work with beryllium. The detection limit is  $0.06 \mu\text{g}$ .

### 3.3. Sampling of airborne dust

The JET vessel is held at a depression and there is air flow through the facility. In vessel airborne sampling was assessed using an air sampler consisting of a cellulose filter paper attached to a pump. The sampler was installed in vessel by remote handling on two distinct occasions after over 580 h of the work during the shutdown: (i) idle, i.e. RH boom was not

operated and retracted into the enclosure, 380 min pumping; (ii) during the RH operation, 360 min pumping. Only results for mass of Be have been processed by the fluorescence method described in Experimental. The levels are below the detection limit, i.e.  $<0.06 \mu\text{g}$ , for both sampling periods. The same result obtained in the absence and presence of in-vessel RH operation clearly indicates low generation rate of air-born dust.

The result indicating very low mobilisation of dust is in agreement with earlier observations made during the initial phase of the shutdown for decommissioning of the TEXTOR tokamak [33, 34]: a carbon wall device in which the generation of dust was regularly surveyed [4, 6, 7]. During the last venting of that vessel a comprehensive search for dust mobilisation was performed. No proof of such process was recorded by several cameras in use. Results of that particular search have not published, but the fact had been noticed.

## 4. Concluding remarks

Until now the examination of dust on the RH equipment has been the only exercise of that kind. The results inform in detail about the character of contamination during a long in-vessel work with many tasks performed. The experiment will be repeated *if* and *whenever* possible and certain modifications and improvements will introduced. Already with the current set of data one can talk about a truly new insight and valuable contribution into at least two areas of dust research: (i) assessment of hazards related to particles' mobilisation in RH operation and (ii) aid in critical view and formulation of conclusions regarding the origin of matter retrieved from tokamaks.

The study confirms earlier experimental evidence that Be-rich co-deposits (and also W coatings on CFC) adhere well to PFC [22, 35]; this is consistent with a small amount of dust found in the JET divertor by vacuum cleaning,  $\sim 1 \text{ g}$  per campaign of 20 h plasma operation. Recent findings also fully clarify a long-standing issue for a source of aluminium (and some other species) in dust samples retrieved from the JET divertor by vacuum cleaning. It has become evident that in-vessel activities generate particulates. Full statistical analysis could not be performed for reasons explained in sections 2 and 3.1, but the examination of all samples has clearly revealed that the accumulation of the most 'fearsome' species, i.e. Be and W, was negligible. Very few small pieces of W from the coatings and only one Be-rich flake from peeled-off co-deposits have been detected.

## Acknowledgments

This work has been carried out within the framework of the EUROfusion Consortium and has received funding from the Euratom research and training programme 2014–2018 and 2019–2020 under grant agreement No. 633053. The views and opinions expressed herein do not necessarily reflect those of the European Commission. The work has been partly supported by

the Ministry of Science and Higher Education of Poland from financial appropriations for science granted for the implementation of the international co-financed project and also by the Swedish Research Council (VR), Grant 2015–04844.

## ORCID iDs

M Rubel  <https://orcid.org/0000-0001-9901-6296>

A Widdowson  <https://orcid.org/0000-0002-6805-8853>

## References

- [1] Winter J 1998 *Plasma Phys. Control. Fusion* **40** 1201
- [2] Winter J and Gebauer G 1999 *J. Nucl. Mater.* **266–269** 228
- [3] Sharpe J P, Chappuis P and Petti D A 2001 *Fusion Technol.* **39** 1061
- [4] Rubel M *et al* 2001 *Nucl. Fusion* **41** 1087
- [5] Balden M *et al* 2014 *Nucl. Fusion* **54** 073010
- [6] Ivanova D *et al* 2009 *Phys. Scr.* **T138** 014025
- [7] Fortuna-Zaleśna E *et al* 2014 *Phys. Scr.* **T159** 014066
- [8] Linke J *et al* 2001 *Phys. Scr.* **2001** T91
- [9] Coad J P *et al* 2018 *Fusion Eng. Des.* **138** 78
- [10] Coad J P *et al* 2001 *J. Nucl. Mater.* **290–293** 224
- [11] Coad J P *et al* 2003 *J. Nucl. Mater.* **313–316** 419
- [12] Rubel M *et al* 2003 *J. Nucl. Mater.* **313–316** 321
- [13] Matthews G F *et al* 2009 *Phys. Scr.* **T138** 014030
- [14] Matthews G F *et al* 2011 *Phys. Scr.* **T145** 014001
- [15] Merola M *et al* 2014 *Fusion Eng. Des.* **89** 890
- [16] Neu R *et al* 2013 *J. Nucl. Mater.* **438** S34
- [17] Endstrasser N *et al* 2011 *J. Nucl. Mater.* **415** S1085
- [18] Widdowson A *et al* 2014 *Phys. Scr.* **T159** 014010
- [19] Baron–Wiecheć A *et al* 2015 *Nucl. Fusion* **55** 113033
- [20] Fortuna-Zaleśna E *et al* 2017 *Nucl. Mater. Energy* **12** 582
- [21] Fortuna-Zaleśna E *et al* 2017 *Phys. Scr.* **T170** 014038
- [22] Rubel M *et al* 2018 *Fusion Eng. Des.* **136** 579
- [23] Gracia-Carrasco A *et al* 2017 *Nucl. Mater. Energy* **12** 506
- [24] Rubel M *et al* 2017 *Phys. Scr.* **T170** 014061
- [25] Rohde V *et al* 2016 *Nucl. Mater. Energy* **9** 36
- [26] Ratynskaia S *et al* 2011 *Plasma Phys. Control. Fusion* **53** 074009
- [27] Litnovsky A *et al* 2013 *J. Nucl. Mater.* **438** S126
- [28] Tolia P *et al* 2011 *Plasma Phys. Control. Fusion* **58** 025009
- [29] Autricque A *et al* 2018 *Nucl. Mater. Energy* **17** 284
- [30] Skilton R *et al* 2018 *Fusion Eng. Des.* **136** 575
- [31] Kimura Y *et al* 1999 *Wear* **232** 199
- [32] Widdowson A *et al* 2016 *Phys. Scr.* **T167** 014057
- [33] Weckmann A *et al* 2017 *Phys. Scr.* **T170** 014053
- [34] Weckmann A *et al* 2018 *Nucl. Mater. Energy* **17** 83
- [35] Jezu I *et al* 2019 *Nucl. Fusion* **59** 086009